Solid State Sciences 67 (2017) A1–A14

Contents lists available at ScienceDirect

Solid State Sciences

journal homepage: www.elsevier.com/locate/ssscie

The use of graphene based materials for fuel cell, photovoltaics, and supercapacitor electrode materials

Alpha C.H. Tsang, Holly Y.H. Kwok, Dennis Y.C. Leung*

Department of Mechanical Engineering, The University of Hong Kong, Hong Kong

ARTICLE INFO

Article history:
Received 10 January 2017
Accepted 7 March 2017
Available online 30 March 2017

Keywords:
Graphene
Fuel cell
Battery
Capacitor
Solar cell

ABSTRACT

This manuscript presents the methodology of the production of 2D and 3D graphene based material, and their applications in fuel cell, supercapacitor, and photovoltic in recent years. Due to the uniqueness and attractive properties of graphene nanosheets, a large number of techniques have been developed for raw graphene preparation, from a chemical method to a physical deposition of carbon vapor under extreme conditions. A variety of graphene based materials were also prepared from raw graphene or graphene oxide, including the metal loaded, metal oxides loaded, to the foreign elements doped graphene. Both two-dimensional (2D) to three-dimensional (3D) structured graphene were covered. These materials included the bulk or template hybrid composite, containing graphene hydrogel, graphene aerogel, or graphene foam and its derived products. They were widely used in green energy device research, which exhibited strong activity, and developed some special usage in recent research.

1. Introduction

Graphene is a two dimensional (2D) structured allotrope of carbon. It deviates from the giant covalent 3D structure of graphite, which is a single-layer crystal composed of sp^2 carbon atoms with hexagonal honey comb shaped carbon ring arrangement [1,2].

Research in graphene and related materials is a hot area in recent years, from the field of physics to chemistry and engineering. A major reason for the strong attention by different groups was its unique and special properties which cannot be replaced by other carbon based nanomaterials. First of all, the electrical conductivity of graphene is very strong with a value of 10^6 S cm^{-1} [3], strong electrical mobility of 200 000 cm^2 V^{-1} s^{-1} at a carrier density of ~10^{12} cm^{-2} [4]. Secondly, it has a high theoretical specific area of 2630 m^{-2} g^{-1} [5], Young's module value of 1 TPa with a breaking strength of 42 N m^{-1} [6], and excellent thermal conductivity (~5000 W m^{-1} K^{-1}) [7]. Thirdly, graphene can also absorb light with board wavelength (~2.3% opacity) which makes it transparent and suitable for optoelectric applications [8]. Finally, graphene has a special reactivity towards different materials, which is one of the most important properties it possess. All these properties are very important for different fields of applications like electrical, electronic, optoelectric, mechanical, environmental, and chemical engineering researches.

Because of the highly attractive properties of graphene mentioned above, various kinds of graphene based products were synthesized. Till date, 2D structured graphene nanosheets (GNs) were extensively prepared and studied. Variety of graphene products ranging from metal to metal oxide, loaded graphene and doped graphene, occupied a large proportion of the study. This also showed the strong ability of GNs to act as building block materials. As a result, 3D porous structured Graphene foam (GF), Graphene hydrogels (GH), and Graphene aerogel (GA), have become a new focus in recent years, among different groups. GF, GH, and GA based materials were extensively studied as it can exist as bulk blocks or porous template hybrid structure in the as-prepared products or modified samples. This can widely extend the range of applications for such materials.

Even though huge effort and extensive works have been inputted to the graphene based green energy research, till date, most of them are still at the fundamental level. Report on the real application level was rare or not even reported. Among them, applications in the fuel cell, and supercapacitor occupied a large portion. Applications in the photovoltics and Li-battery were new directions of graphene. Most of the works were done through traditional ways involving dispersion of GNs, GH, or GA based materials in solvent or liquid reactant before the start of reactions, and some even needed pretreatment of samples. This can ensure

* Corresponding author.
E-mail address: ycleung@hku.hk (D.Y.C. Leung).

http://dx.doi.org/10.1016/j.solidstatesciences.2017.03.015
1293-2558/

that all surfaces of the graphene based material come into contact with the reactants, especially for the 2D GNs. However, it may also be disadvantageous to 3D graphene based materials due to the risk of 3D porous structure destruction, and the reduction in the active surface area due to the use of binders. These problems made them almost no different from the 2D GNs. As a result, the performance of the processed GH or GA catalyst may be masked. In order to reflect the true power of the 3D graphene based catalyst, extensive works have been done in recent years. These works were the direct use of GH or GA, cutting bulk GA/GH into disc, or preparing the GH or GA hybrid structures on an inert template, especially metallic microporous template. This technique had the strength to keep the 3D GA or GH skeleton. In addition, the electroconductivity of the GA can be enhanced through better electric contact between the GNs in the GA or GH and the metallic microporous materials. Most importantly, no binder was required, which is convenient to use in a real device application.

Even though there are reviews focused on the energy production of graphene based materials, such as raw graphene oxide (GO), or 2D and 3D graphene based materials [9–11]. The focus was still mainly on the specific groups of traditional graphene materials. The applications of such materials in green energy and environmental research are usually in specific manner [10,11]. It is still of interest to have a review on some new techniques and corresponding applications which developed very recently.

In this manuscript, an integrated review was conducted on 2D and 3D based graphene materials preparation, and their green energy application. Several sections are included in this manuscript, where the preparation of the raw graphenes and their challenges in recent year is the starting section. Second section is focused on the variation forms of graphene, from 2D to 3D structured products, and metal, metal oxides and foreign elements loaded products. The roles and activity of graphene based products in fuel cell, supercapacitors, lithium battery and photovoltics materials is the core area in third part. The challenges on the use of graphene based material in green energy devices will be discussed as the final section.

2. Graphene based materials preparation

2.1. Raw graphene oxide

There are three common methods for synthesizing raw graphene. First, graphene can be directly prepared on substrate by Chemical Vapor Deposition (CVD) [12,13]. This method involves the use of a volatile carbon source such as ethanol, and a carrier gas under extra high vacuum environment, to produce high quality graphene products. However, this method suffers from the requirement of an extreme reaction condition and the use of a toxic carrier gas. This make the production unfriendly to the environment. In addition, the surface area of the graphene produced is also limited by the small surface area of the substrate [12,13]. As a result, such graphene is most suitable for direct fabrication of small devices. The second way of graphene preparation is the exfoliation of graphite through oxidation, or so called Hummer's method [14], which is a common method for graphene synthesis in a bulk quantity manner. Graphite can be directly oxidized and exfoliated into graphene oxide by oxidizing the graphite with strong oxidizing agents like potassium permanganate ($KMnO_4$) [14]. However, both the yield and quality of the graphene produced are not good in this manner due to the formation of graphite-core/GO shell structure in the final product [15]. As a result, modified Hummer method was proposed to improve the quality of graphene in the recent years [15–24]. The first step of this method is to convert graphite to pre-oxidized graphite via peroxidation. This involved the use of a strong oxidizing agent like phosphorus pentaoxide (P_2O_5) and potassium persulphate ($K_2S_2O_8$) in the traditional Hummer's reaction, or using a mild reagent (such as sodium nitrate ($NaNO_3$), and sodium citrate) in the graphite preoxidation step [19–22], under the so called Hummers and Offenman's method [23,24]. Preoxidized products were obtained after the neutralization and drying process [15–24]. The pre-oxidized graphite is further oxidized by permanganate ion with quenching by hydrogen peroxide (H_2O_2) solution. The final product can be obtained by a series of dilute HCl cleaning and dialysis in deionized water (DI water), followed by freeze frying of samples, or direct storage without treatment [25–29]. Drying can be done via a pure liquid GO [30], drying in an oven under vacuum or ambient condition [31,32], or in air [19,33]. The cleaned product usually has stability for years [15]. The bulk GO or GO on Nickel Foam (GO/NF) can then be reduced into graphene (GNs) or (3D-NiGO: NF supported GO) by using reducing agents [34–38], heating the GO [39], or just keep under ambient environment [40].

Even though Hummer's method based synthesis of GO is simple with high yield, its stability has been discovered not high at weekly to monthly basis. GO was found unstable at an elevated temperature of 50 °C [41,42], and metastable at room temperature [43]. The major reason was due to the existence of defects exhibited from some functional groups like carboxylate group from the oxidation step [42], which resulted in the formation of hole defects due to the CO_2 elimination [44]. Consequently, this becomes the barrier of high quality GO production and made the synthesis of a stable GO a challenge. Recently, Eigler et al. [41] successfully prepared GO with higher stability by modifying the Hummer's method. In the modified method, the reaction temperature was reduced from 35 °C in classic version of the $KMnO_4$ oxidation step to 10 °C with the extension of reaction time up to 16 h [41]. This method claimed to be one of the solution for reduction of the defects in order to improve the quality of GO.

Generally, 3D graphenes are divided into several forms, including free standing graphene hydrogel (GH), graphene aerogel (GA), and the graphene foam (GF). Strictly speaking, GH and GA belong to the same category of materials, as the space inside GH is water or crosslink agents, while GA is the dried form of GH after removal of the spatial water. The most common method for the GH/GA preparation is the chemical reduction of the exfoliated aqueous GO dispersion through the use of a reducing agent in close system under heating in an oven. N_2H_4, $NaBH_4$, amine based compounds, hypophosphorous acid, iodine, or formaldehyde were common reducing agents for hydrothermal reduction in GH/GA preparation [45–50]. However, the GH produced from such reducing agents usually needs extreme conditions like high temperature, even though the time needed is short. Most importantly, the reducing agents used are toxic in nature, which are not environmentally friendly. As a result, non-toxic reducing agents are adopted as the alternatives in recent years. The most commonly used green reducing agents in recent years include VC (L-ascorbic acid or Vitamin C), ethylene diamine, both of which are used in the synthesis of free standing GA [16,19,25,47,51] and supported GA like GA/NF [19]. Fig. 1 showed the digital images and SEM images of GA/NF. The black GA covered the surface of the NF, and was embedded in the NF skeleton throughout the reduction [19]. Besides the use of reducing agent, the GA or GA/NF can also be synthesized by reducing the GO aerogel or GO/NF formed on NF in inert gas annealing [20,52], exposure to an extremely low temperature environment [20,53], or hydrothermal reaction in the absence of a reducing agent [54].

In general, pure GA can be successfully synthesized from GO with a corresponding concentration in the range of 0.4–15 mg mL^{-1} [19,25,45,47,55–57]. Hu et al. [47] observed that pure GA could not be obtained when the initial GO concentration

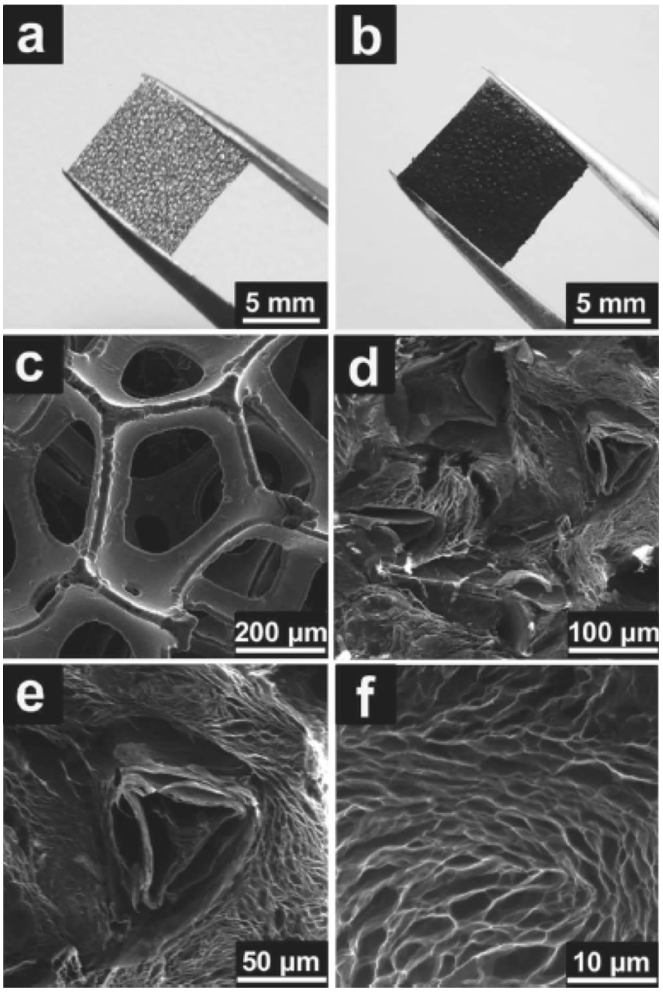

Fig. 1. Photographs of (a) piece of NF and (b) as-formed G-Gel/NF electrode. (c) A SEM image of NF. (d, e) Cross-sectional SEM images of freeze-dried G-Gel/NF electrode at different magnifications. (f) A magnified SEM image of G-Gel in G-Gel/NF. (reproduced with permission from WILEY-VCH Verlag GmbH & Co. [19]).

was lower than 2 mg mL^{-1}. The density of pure GA obtained was also increased upon the increased in the GO concentration from 3 mg mL^{-1}. However, some of the cases showed that pure GA can still be formed when the GO concentration was smaller than 2 mg mL^{-1} [56,57]. The size of the GA obtained from their group was increased when the concentration of GO used increased [56]. The main difference may be due to the difference in the nature of GA synthesis. In Lim's group, the GA was prepared from the hydrothermal reaction at high temperature without the use of reducing agent [56]. In contrast, those from another studies involved the use of reducing agent with different reducing power [19,25,45,47,55]. In the case of hydrothermal reaction without the use of reducing agent, the GA formation was done through the Van del Waal's force and hydrogen bond between GO nanosheets and water molecules [57]. However, pure GA synthesis in the presence of reducing agent was done through the restoring of the π-π interaction between the GO sheets in order to carry out the gelation for GH formation [25]. In addition, some of the reducing agent like toxic N_2H_2, $LiAlH_4$ and $NaBH_4$ may produce gaseous products, while some of them like EDA and VC did not throughout the GH formation [25,47]. This may be resulted in the cracked GH produced due to strong bubbling [47]. Consequently, the initial concentration of GO and type of reducing agent may then control whether GH/GA can be formed, its quality, and mechanical properties of pure GH/GA when different method was used.

In the case of GF, it is commonly prepared by two different pathways. The first pathway is the preparation of ordinary 2D graphene films on the surface of nickel foam (NF), through the CVD approach, followed by the removal of NF support by hydrochloric acid [58–61]. Another method is similar to the CVD's pathway, which replaces the CVD step by soaking the NF in GO dispersion, or by mixing GO with carbon nanotubes as the first step, followed by the reduction of GO into graphene nanosheet film on the supporting materials [62]. Direct preparation of GF from graphite paper is another recent direction. It is done through the oxidation of graphite paper (GP) into graphene oxide paper (GOP) by Hummer's method, followed by freeze drying of GOP and N_2H_4 reduction into GF, which is similar to the conventional 2D GO preparation [63]. GF can also be prepared in tube furnace via the use of ammonium and urea based precursors under high temperature in a closed inert system [64].

2.2. Metal loaded graphene based nanostructures

Till date, there are several pathways for producing both M/GNs (2D) and M/GH or M/GA (3D). First of all, direct reduction of a metal ion/GO mixture by a reducing agent with heating is the most common method, no matter whether it is monometallic or polymetallic M/GNs, or M/GHs and M/GAs [16,26–29,32,39,48,65–99]. For monometallic M/GNs, single metal salts (Pd, Pt, Au, Ag, Ni based) and dispersed GO are mixed together with a reducing agent under vigorous stirring as the first step. This is followed by either hydrothermal reduction in an autoclave [75,83], reduction in a microwave oven [71,74], direct reduction through mixing and heating in ambient environment [26–29,39,70,72,73,82,87,100,101], or through displacement reaction between metal ions [100,102] under an inert [103] or carbon monoxide (CO) environment [23]. Some of the cases were done under reflux condition [28,95,96], or even just through direct mixing between GO and metal ions with heating [104–109]. For bimetallic M/GNs, some of the cases were done through direct mixing under heating in ambient environment [26–29,32,39,76,85,93,104,110], or under a CO environment [35]. However, no stirring was required for the preparation of 3D M/GA or M/GH based materials [16,48,97,99]. The reduced mixture was cleaned through a centrifuge in deionized (DI) water [39,105], freeze drying of the cleaned solution [26,28], or direct drying in an oven or ambient air [32,72,73,83,93,95,96]. For common cases, borohydride ions (BH_4^-), hydrazine (N_2H_4), or amine based species was used as a reducing agent for the M/GNs preparation as listed in Table 1 [27,32,48,63,65,66,70,72,77,78,81,82,84,85,87,88,92,95,97,99]. However, such reducing agents are also highly toxic in nature which is unfriendly to the environment. As a result, green reducing agent becomes an alternative choice in the recent research. L-ascorbic acid or so called vitamin-C (VC), ethanol, ethylene glycol (EG), polyols like 1,2-propanediol (PD), or formic acid were commonly used green reducing agent [16,26,28–30,36,39,67–69,71,73–76,79,86,89–91,93,94,96], which is also summarized in Table 1. The quality of the resulting M/GNs synthesized was similar to those from the BH_4^- reduction [26,28]. Fig. 2 showed the digital images and preparation scheme of Au/GH through the hydrothermal process, which was a black block in shape [98].

Other than chemical reduction, electrodeposition of metal ions on graphene is another approach for the M/GNs synthesis [24,31,33,111–117]. Graphene used in such preparation was coated on a secondary substrate like carbon fibre paper, glassy carbon electrode, ITO glass, or gold electrode. The supported graphene was then put into an aqueous monometallic or bimetallic solution, and

Table 1
List of the commonly M/GNs and M/GH or M/GA synthesized by reduction, types of reducing agent, and surface properties.

M/GNs	Reducing agent (Green/Toxic)	Electochemical active surface area ($m^2\ g^{-1}$)	Ref
Pd/GN1, Pd/GN2	BH_4^- (Toxic)	182.56 (Pd/GN1), 162.56 (Ps/GN2)	[32]
Pd/RGO, PdRu/RGO, PdSn/RGO, PdIr/RGO	BH_4^- (Toxic)	58.1 (Pd/RGO), 52.0 (PdRu/RGO), 64.9 (PdSn/RGO), 61.6 (PdIr/RGO)	[27]
Pt/Graphene	BH_4^- (Toxic)	141.6	[72]
Pt/Graphene	BH_4^- (Toxic)	44.6	[77]
Pd_1Ni_1-NNs/RGO, Pd/RGO	BH_4^- (Toxic)	98.2 (Pd_1Ni_1-NNs/RGO), 67.2 (Pd/RGO)	[81]
Pd-Au (1:1)/RGO, Pd/RGO	BH_4^- (Toxic)	N/A	[84]
Pd-Ag (1:1)/RGO-SB	BH_4^- (Toxic)	N/A	[85]
G-Pd, G-Pt	BH_4^- (Toxic)	3.52 cm^2 (G-Pt), 0.12 cm^2 (G-Pd)	[87]
Pt/graphene	BH_4^- (Toxic)	98	[95]
Pt@Pd/RGO, Pt/RGO, Pd/RGO	N_2H_4 (Toxic)	15.11 (Pt@Pd/RGO), 10.42 (Pt/RGO), 10.59 (Pd/RGO)	[65]
Pd-Pt ANFs/RGO	N_2H_4 (Toxic)	200.32	[66]
Ni/rGO	N_2H_4 (Toxic)	N/A	[70]
Pd/Cu/graphene	N_2H_4 (Toxic)	20.22	[78]
Gra/Pd	N_2H_4 (Toxic)	47 cm^2 (0.25 cm^2 geometric surface area)	[88]
PtPd NFs-RGO	N_2H_4 (Toxic)	26.33	[92]
PdRGO	Oleylamine (Toxic)	N/A	[82]
GA	BH_4^-(Toxic)	N/A	[48]
3DGFs	N_2H_4 (Toxic)	N/A	[63]
Ni/graphene aerogel	N_2H_4 (Toxic)	N/A	[97]
Au/graphene hydrogel	Triethylenetetraamine(Toxic)	N/A	[98]
Pd/3DGA	BH_4^- (Toxic)	N/A	[99]
Pd@Pt/RGO, PdPt/RGO	L-ascorbic acid (Green)	29.94 (Pd@Pt/RGO), 37.55 (PdPt/RGO)	[26]
Pd/graphene, Pt/graphene, Au/graphene, Ag/graphene	L-ascorbic acid (Green)	N/A	[28]
Au@Pd-G, Au-G, Pd-G	L-ascorbic acid (Green)	N/A	[67]
RGOs-PtPd NHs	L-ascorbic acid (Green)	18.5	[68]
Pt1Pd3NPs/G, PtNPs/G, PdNPs/G	L-ascorbic acid (Green)	23.34 (Pt1Pd3NPs/G), 21.93 (PtNPs/G), 13.87 (PdNPs/G)	[69]
PdNCs/G, PdNPs/G	L-ascorbic acid (Green)	50.28 (PdNCs/G), 25.64 (PdNPs/G)	[79]
PtPd/RGO, Pt/RGO, Pd/RGO	L-ascorbic acid (Green)	83.1 (PtPd/RGO), 16.3 (Pt/RGO), 12.5 (Pd/RGO)	[89]
PtNFs-GO	Ethanol (Green)	72.1	[29]
PtPdNPs/GNs, PdNPs/GNs, PtNFs/GNs	Ethanol (Green)	0.54 cm^2 (PtPdNPs/GNs), 0.17 cm^2 (PdNPs/GNs), 0.25 cm^2 (PtNFs/GNs)	[39]
40%Pd–10% Ru/GNS, Pd/GNS	EG (Green)	99 cm^2 (40%Pd–10% Ru/GNS), 100 cm^2 (Pd/GNS)	[36]
Pt/CCG	EG (Green)	36.27	[73]
Pt/ND/G-1500, Pt/ND/G-1200	EG (Green)	137.9 (Pt/ND/G-1500), 125.1 (Pt/ND/G-1200)	[74]
GNP/Pt, RGO/Pt	EG (Green)	63.0 (GNP/Pt), 53.6 (RGO/Pt)	[75]
Pd-Ag/RGO, Pd/RGO, Ag/RGO	EG (Green)	N/A	[76]
Pd-Cu/RGO, Pd/RGO, Cu/RGO	EG (Green)	N/A	[86]
Pd-CuNC/RGO	EG (Green)	49.2	[90]
Gr-Pd, Gr-Pt	EG (Green)	544.3 (Gr-Pd, BET), 478.3 (Gr-Pt, BET)	[94]
Pt/GNP	EG (Green)	~40	[96]
Pt/GO-5, Pt/GO-10	PD (Green)	85.71 (Pt/GO-5), 65.61 (Pt/GO-10)	[71]
PdPt@Pt/rGO, PtPd/rGO, Pt/rGO, Pd/rGO	Formic acid (Green)	58.9 (PdPt@Pt/rGO), 20.5 (PtPd/rGO), 17 (Pt/rGO), 14 (Pd/rGO)	[91]
G-PtPd, G-Pt	Formic acid (Green)	38.6 (G-Pt), 23.6 (G-PtPd)	[93]
Pd/GA/NF	L-ascorbic acid (Green)	N/A	[30]
RGO/Pt hybrid hydrogel	L-ascorbic acid (Green)	N/A	[16]

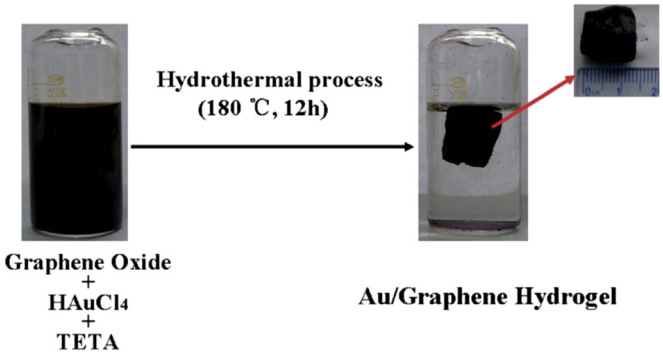

Fig. 2. Digital image presentation of Au/GH synthesis throughout hydrothermal reduction (reproduced with permission from RSC [98]).

deposited through the traditional cyclic voltammetry in a 3-electrode system for few tens to hundreds of seconds [24,31,33,111,112,114–117]. In the case of metal loaded 3D graphene structures, GF produced through CVD was used as catalyst carrier [59]. The GF synthesized from graphene deposition on NF through CVD, followed by the removal of NF by strong acid can act as working electrode for the metal deposition in metal solution ($PtCl_6^-$) [59]. In some of the cases, the M/GNs product was obtained by electrochemical milling of the metal (Pd) wires coiled graphite rod, which were acted as both working and counter electrode in the electrolyte like sulphuric acid under an AC supply. The final product was then obtained through centrifuge of the acid dispersion [113]. Also, the M/GNs can be electrodeposited onto substrates like ITO glass through the use of a M/GO (Pt/RGO) solution as deposition solution [115]. For the graphene prepared through CVD, the M/GNs is mainly prepared through sputtering [12]. Recently, ultra-sonication is a new pathway for the M/GNs preparation [118–120].

2.3. Metal oxide loaded graphene based nanocomposites

Generally, the preparation of 2D MO_x/GNs and MO_x loaded 3D graphene (MO_x/GH, MO_x/GA, or MO_x/GF) was similar to that of the M/GNs and M/GA. The only difference is the additional further treatment of M/GNs synthesized from the M/GO mixture reduction [121–128], or direct reduction of MO_x/GO mixture [58,61,129–132]. In the first case, reaction between metal and graphene through chemical reduction or solvothermal reactions, metal salts (titanium (IV) isobutoxide ($Ti[(CH_3)_2CHCH_2O]_4$) [133], $TiCl_3$ [128], $TiCl_4$ [124], $KMnO_4^-$ [123], $Zn(NO_3)_2 \cdot H_2O$ [122], $Zn(OAc)_2$ [126], $Zn(NO_3)_2$ [125],

or $SnCl_2 \cdot 2H_2O$ [127]) is directly mixed with an exfoliated GO dispersion before further reaction. In the case of direct reaction between MO_x and GO, the MO_x source is either separately prepared from a metal salt [58,61,129] or from a market available product (such as P25) [130]. Besides the chemical pathway, electrochemical method is another approach for the 2D MO_x/GNs formation [122,134,135].

Other than the chemical pathways, ultrasonic preparation through direct mixing of MO_x or metal precursor with GO or GO/polymer is also a feasible pathway, which is more convenient for producing 2D MO_x/GNs or 3D MO_x/GF [129,136].

2.4. Foreign element doped graphene based nanostructures

Other than the metal and metal oxides loaded graphene based products, non-metallic foreign element doped graphene based materials is also a popular material in recent years [13,137–150]. In general, such nanocomposites can be prepared by two approaches. The first one is the CVD method for 2D graphene. It is done by reacting the as-prepared 2D GNs on a substrate through CVD pathway under the flow of ammonia gas in the CVD system [13,142]. Another pathway is the chemical reaction. The mono-elements doped or codoped 2D GNs and 3D GA products can be prepared through a chemical pathway by mixing GO and dopant containing compounds with heating, followed by reduction, with a reducing agent or under direct heating [138,140,141,143–148]. The only difference is the 2D graphene based materials needs continuous stirring of the GO/dopant mixture throughout the synthesis, while in the 3D graphene's preparation stirring is not required in the hydrothermal reaction step. Some of the B-doped, N-doped or BN co-doped 2D GNs can also be synthesized by a green pathway by direct mixing of a boron source. Such as boric acid, sequential addition of boric acid and NH_3, or boron and nitrogen coexisting compounds in the absence of a reducing agent, followed by heating at high temperature in an inert gas environment [137,149,150]. In addition, the dopant itself also acts as a reducing agent in the foreign element doped GA preparation [143,144]. In recent years, one-step direct growth of foreign element (N) doped graphene hydrogel on secondary substrate was also developed. The procedure was similar to that of the GA/NF or GH/NF, and M/GA/NF, the only difference is the reactant (urea) was added in the hydrothermal reaction step after the NF soaked with the GO dispersion [147].

Similar to pure GA described in the previous section, foreign element doped GA can be prepared with varying GO concentration in the range of 0.2–5 mg mL^{-1} [57,144,145]. The reason behind for the lower initial GO concentration is due to the fact that the formation of foreign element doped GH is done through the π-π interaction and Van del Waals force between the GO sheets and the dopant during the gelation process [57,145]. Besides the chemical reduction, electronic doping of GO with dopant like NH_3 by high power electrical annealing is an alternative preparation option for the foreign element doped GNs [139].

Besides the bulk foreign element doped GH or GA, 3D structured graphene can also be in powder form. One of the example is the B-doped 3D graphene, synthesized by Zhou et al. [146], through the reaction between the freeze dried GO and borane trimethylamine as dopant under heating in a CO_2 environment.

3. Applications of graphene based materials in green energy devices

3.1. Fuel and electrochemical cells

In the era of fossil fuel crisis, development of alternative energy with low emission and high energy conversion efficiency, relative to traditional fossil based energy source becomes a challenge. The use of electrocatalyst is one of the directions. Till date, most of the research in this direction involves the use of metal catalysts. Alcohols, including methanol and ethanol electrooxidation (MOR and EOR), occupied a large proportion among them, some of them were also investigated for the ability of glucose oxidation. This type of fuel is regarded as one of the most abundant biofuels derived from natural crops and food waste. The Pt based GNs catalyst was most commonly used in the electrooxidation in past years. The Pt/GNs showed strong catalytic activity in acidic or alkaline MOR and EOR when compared to traditional Pt/C catalyst. This is reflected by the strong anodic sweep current density (J_f) of 2540 A g^{-1} [26], or 30 mA cm^{-2} [73] and high toxic tolerance (I_f/I_b) value of 6.6 [68] when compared with the commercial Pt/C, Pt black or Pt on different support in MOR, which resulted in an anodic sweep current density as high as 26.7 A g^{-1} [91], or 12 mA cm^{-2} [89] and I_f/I_b ratio as high as 4.84 [91] in EOR. Table 2 summarized the different J_f and I_f/I_b values obtained from different Pt loaded graphene based electrocatalysts in MOR and EOR [26,29,33,39,65,66,68,69,71–75,77,87,89,91,103,104,116,117]. The use of 3D structured graphene has become a new focus in recent years, because it has 3D porous structure in the 3D graphene structured backbone which provides large surface area for loading catalyst, and exhibits superior electroconductivity compared to 2D GNs. More importantly, the free standing type 3D graphene catalyst or 3D graphene/porous structures hybrids nanocomposites can be used as direct catalyst without the need of any treatment, which is very important for green catalyst development. In record, monometallic platinum loaded GF was studied, which showed strong electrocatalytic activity in anodic alcohol oxidation. In the study conducted by Maiyalagen et al. [59], free standing Pt/GF showed strong performance in the methanol oxidation in acidic media, with high current density (1.6 mA cm^{-2}) which doubles that produced from normal carbon fiber template catalyst (0.8 mA cm^{-2}) [59].

Due to the weakness of monometallic Pt nanocatalyst that suffers from the CO poisoning after prolong service in alcohol electrooxidation, alternative metallic catalysts, such as monometallic Pd, Ni, and bimetallic M/GNs or M/GA were developed [24,26,27,35,60,65–70,76,78,80,81,83,85,87,88,90–92,97,99,100,104,

Table 2
List of the J_f, I_f/I_b in the Pt/GNs catalyzed MOR and EOR.

M/GNs catalyst	Type of oxidation	J_f (Anodic sweep)	I_f/I_b	Ref
Pt/rGO	MOR	2540 (mA mg^{-1})	4.19	[26]
Pt/NFs-GO	MOR	523 (mA mg^{-1})	1.2	[29]
GO/Pt	MOR	0.987 (mA cm^{-2})	1.37	[35]
Pt/rGO	MOR	16.53 (mA cm^{-2})	3.31	[65]
Pt NF/rGO	MOR	1.77 (mA cm^{-2})	2.52	[66]
rGO/Pt	MOR	0.88 (mA cm^{-2})	6.6	[68]
PtNPs/G	MOR	1.688 (mA cm^{-2})	5.63	[69]
Pt/GO	MOR	590 (mA mg^{-1})	1.03	[71]
Pt/graphene	MOR	2.53 (mA cm^{-2})	1.92	[72]
Pt/CCG	MOR	30 (mA cm^{-2})	0.83	[73]
Pt/ND/G	MOR	98.7 (A g^{-1})	0.93	[74]
rGO/Pt	MOR	44.2 (mA cm^{-2})	0.85	[75]
GNP/Pt	MOR	57.7 (mA cm^{-2})	1.21	[75]
Pt/graphene	MOR	199.6 (mA mg^{-1})	1.06	[77]
G-Pt	MOR	0.455 (mA cm^{-2})	1.93	[87]
Pt/rGO	MOR	23 (mA cm^{-2})	3.61	[89]
Pt/GNs	MOR	22.9 (mA cm^{-2})	2.23	[103]
Pt PNWs/rGO	MOR	394 (mA mg^{-1})	0.99	[104]
Pt/EGS	MOR	7.41 (mA cm^{-2})	1.78	[116]
Pt NPs@G	MOR	195 (mA mg^{-1})	1.26	[117]
Pt/Nf-graphene	EOR	2.28 (mA cm^{-2})	1.05	[33]
PtNF/GNs	EOR	9.1 (mA cm^{-2})	0.99	[39]
Pt/rGO	EOR	12 (mA cm^{-2})	N/A	[89]
Pt/rGO	EOR	26.7 (mA mg^{-1})	4.84	[91]

106,114,119,120]. Some of these studies are listed in Table 3. They can be used for a wider range of fuel oxidation, such as ethanol [24,27,33,39,60,78–80,84–89,91,92,97], glucose [105,111], and formic acid [32,81–83,102,113] when compared to Pt/GNs and Pt loaded 3D graphene. Results from different groups showed that monometallic Pd, Ni, and bimetallic Pd or Pt based electrocatalysts have enhanced electrocatalytic activity with a strong tolerance towards CO poisoning when compared with the monometallic Pt/GNs. Major evidence was the high anodic peak current density produced (4972 A g^{-1} [26] or 252 mA cm^{-2} [89] in MOR, 2105.4 A g^{-1} [86] or 2219 mA cm^{-2} [84] in EOR) and the high I_f/I_b ratio (11.65 in MOR [86] and 5.45 in EOR [33]) from such catalysts were larger than that of monometallic Pt/GNs. Corresponding values for monometallic/GNs or bare Pd and Pt based catalyst in alcohol oxidation were summarized in Table 4. In addition, the stability of such catalysts were also high, as the value of the anodic peak current density can keep constant over 25 to 500 cycles in CV tests or low decay rate of current density in chronoamperometry [24,26,27,35,36,39,65–70,76,78–80,83–89,91,92,100,104, 106,114,119,120]. In the GA based EOR or MOR studies, the performance of non-Pt electrocatalyst was comparable to the Pt based catalyst. For example, Ren et al. [97] has investigated the Ni/GA performance in the electrooxidation of ethanol, under different scanning rate and ethanol concentration. The finding reflected that Ni/GA's performance was enhanced upon the increase in the scanning rate and concentration of ethanol. The current density of fully activated Ni/GA recorded, was 16.3 mA cm^{-2} [97]. While Liu's group found that the Pd/GA catalyzed methanol oxidation resulted in a current density of 8 A mg^{-1} with I_f/I_b ratio of about 1.2 [99]. Another study carried out by Kung et al. [60] involved the use of bimetallic PtRu loaded GF as MOR and EOR catalyst in acidic condition. The current density produced at a fully activated cycle was about 110 mA cm^{-2} in MOR and 80 mA cm^{-2} in EOR. It was approximately 2 times larger than that generated from the corresponding 2D GNs based catalyst [60]. Development of one-step binder-free M/GA electrode on NF substrate for electrocatalyst was another direction recently. It is due to the experience gained in the green growth pathway of pure GA on the NF and corresponding application in the supercapacitor testing developed by other groups [19,20]. Tsang et al. [30] has developed a one-step preparation of Pd/GA on NF, which acts as a new type of binder free direct electrode. The results showed that the Pd/GA/NF electrode has stronger performance in the methanol and ethanol oxidation in over 1000 cycles (13–15 h) of CV scanning with the final current density of over 300 A g^{-1} in value. Its toxic tolerance towards CO poisoning ($I_f/I_b = 2–3$) was also stronger than the existing M/GNs (<1) [30]. Even though there is other kinds of low cost nanomaterials based catalyst like silicon nanowire arrays with good performance [151], the use of the toxic chemicals like hydrofluoric acid with metal ions as etchant for the array formation on the silicon wafer surface make the process not friendly to the producer. In addition, series of pretreatment like activation through high temperature annealing make the preparation of electrode complicated [151]. In contrast, the one-step preparation of GA/NF or GH/NF based electrodes by chemical reduction under mild thermal condition is relative easy and safe to operate. This make GA based material still have an advantage over other low cost materials.

Other than alcohol oxidation, non-Pt based GNs catalysts also exhibit strong activity in formic acid oxidation, as reflected from the strong current density of 13.8–61.6 mA cm^{-2} or 210.0–604.3 A g^{-1} [32,81–83,102,113]. The activity of M/GNs in glucose oxidation was also investigated, such reactions were non-Pt based M/GNs catalyzed conducted in alkaline solution. Shi et al. [111] recorded a strong current density of 7.4–16.2 mA cm^{-2} in Au/rGO/GC and Au/Ag/RGO/GC, and the stability of the catalyst was also high, throughout a 500 cycles scanning.

Besides the performance in the anodic half-cell activity, some M/GNs or M/GA driven electrocatalysis also involved oxygen reduction reaction (ORR) alone [90,95,96,109]. Such works were done in acidic solution (such as H_2SO_4 and $HClO_4$) for the Pt based M/GNs and Pd/GA [95,96,109], and in alkaline solution (such as KOH) for Pd based M/GNs [90]. Some of the works were similar to the alcohol oxidations, where the current density was the main focus. The result showed that the ORR current density produced from Pd based bimetallic GNs could reach 38.4–174 mA mg^{-1}, which was approximately 2 and 15 times larger than that of rGO and bare Pd black, respectively [90,119]. Also, the M/GA also showed strong activity in the ORR reactions in acidic media, which is reflected by the high onset potential (+0.65 V) from the study conducted by Yun's group [109]. It is comparable to the commercial Pt/C catalyst (+0.8 V), but the mass activity of Pd/GA was stronger, which made Pd/GA the best [109]. Another focus of the M/GNs catalyzed ORR was the potential of the ORR peaks recorded from linear sweep voltammetry, or the ORR over potential, which either showed low rate of half wave potential decrease, or onset potential and half wave potential shifted to more positive value with strong durability (44–120 h) for the Pt/GNs, Pd/GNs or bimetallic Pt or Pd based GNs catalysts when compared with other bare Pt and Pd based catalysts loaded on other supporting materials like carbon black, carbon nanotube (CNT) and XC-72 [35,90–92,95,96,119]. Another group of studies were done with electrooxidations in order to observe the possibility of the catalyst used as both cathodic and anodic materials [35,90–92,105,119]. The results showed that other than the strong ability in the alcohols and glucose oxidation, the ORR activity in either acidic or alkaline solution was also excellent as mentioned above [35,90–92,105,119]. Some of the studies even involved the alcohol-tolerance test where methanol was added to a KOH or $HClO_4$ solution in the ORR [35,90]. The result showed no methanol oxidation signal from CV nor reduction in current density for M/rGO or even the control sample of pure rGO in the presence of methanol throughout the ORR reaction, when compared with the traditional Pt/C. This finding reflected that M/rGO or the control rGO sample had strong selectivity towards ORR even though permeation of alcohol had taken place, and this can avoid the risk of fuel cell damage [35,90]. One of the examples was shown in Fig. 3, where rGOs and the bimetallic Pd-Cu NC/rGOs have strong selectivity towards the ORR in the presence of methanol in O_2-saturated

Table 3
List of commonly used monometallic non-Pt and bimetallic M/GNs based electrocatalyst.

M/GNs	Ref
Pd/GN, PdNCs/G, FS-Pd/GO, Pd/GNP	[24,27,32,33,35,36,39,65–69,76, 79–89,91,100,102,105,106,113,119]
PdPt/rGO	[26,33,35,39,66,68,69,89,91,92,120]
Pd@Pt/rGO	[26,65]
PdPt@Pt/rGO	[91]
PdRu/rGO	[27,36]
PdSn/rGO	[27]
PdIr/rGO	[27]
Au/GNs, Au/rGO	[67,111,119]
Au@Pd/GNs, Pd-Au/rGO	[67,84]
G-AuPD@Pd	[119]
Ag/Au/rGO	[111]
Au/Ag/rGO	[111]
Ni/G	[70]
Ag/rGO	[76]
Pd-Ag/rGO	[76,80,85]
Pd/Cu/graphene, Pd-Cu/rGO	[78,86]
PdNi-NN/rGO	[81]
Cu/rGO	[86]
PtIr PNWs/rGO	[104]
Pt-Co/G	[114]

Table 4
List of the J_f, I_f/I_b in the monometallic non-Pt M/GNs and bimetallic M/GNs catalyzed electroxodation.

M/GNs catalyst	Type of oxidation	J_f (Anodic sweep)	I_f/I_b	Ref
Pd@Pt/rGO	MOR	4972 (mA mg^{-1})	2.10	[26]
PdPt/rGO	MOR	3824 (mA mg^{-1})	2.29	[26]
Pd/rGO	MOR	0.13 (mA m^{-2})	2.10	[27]
PdRu/rGO	MOR	0.17 (mA m^{-2})	2.43	[27]
PdSn/rGO	MOR	0.14 (mA m^{-2})	2	[27]
PdIr/rGO	MOR	0.14 (mA m^{-2})	3.5	[27]
GO/Pd	MOR	0.086 (mA cm^{-2})	N/A	[35]
GO/PdPt-03	MOR	4.35 (mA cm^{-2})	1.16	[35]
40%Pd/GNs	MOR	47 (mA cm^{-2})	5.22	[36]
40%Pd-5%Ru/GNs	MOR	118 (mA cm^{-2})	3.11	[36]
Pd/rGO	MOR	96.11 (mA cm^{-2})	1.92	[65]
Pt@Pd/rGO	MOR	130.37 (mA cm^{-2})	2.3	[65]
Pd NF/rGO	MOR	1.87 (mA cm^{-2})	2.66	[66]
Pd-Pt ANF/rGO	MOR	2.16 (mA cm^{-2})	3.29	[66]
Pd/GN	MOR	0.199 (mA cm^{-2})	N/A	[67]
Au/GN	MOR	0.133 (mA cm^{-2})	N/A	[67]
Au@Pd/GN	MOR	0.663 (mA cm^{-2})	N/A	[67]
rGO/Pd	MOR	0.38 (mA cm^{-2})	5.7	[68]
rGO/Pt-Pd	MOR	28 (mA cm^{-2})	7	[68]
PdNPs/G	MOR	1.157 (mA cm^{-2})	3.21	[69]
Pt_1Pd_3NP/G	MOR	2.272 (mA cm^{-2})	2.52	[69]
Ni/G	MOR	20 (mA cm^{-2})	N/A	[70]
LDG/Pd	MOR	27.6 (mA cm^{-2})	6.62	[83]
rGO/Pd	MOR	15.0 (mA cm^{-2})	4.5	[83]
Pd/rGO	MOR	360.79 (mA cm^{-2})	4.33	[84]
Pd-Au/rGO	MOR	1218.43 (mA cm^{-2})	1.12	[84]
Pd/rGO	MOR	311 (mA mg^{-1})	1.41	[85]
Pd-Ag/rGO	MOR	630 (mA mg^{-1})	3.15	[85]
Pd/rGO	MOR	358.5 (mA mg^{-1})	11.65	[86]
Cu/rGO	MOR	0 (mA mg^{-1})	N/A	[86]
Pd-Cu/rGO	MOR	1153.4 (mA mg^{-1})	2.88	[86]
G-Pd	MOR	0.7875 (mA cm^{-2})	16.7	[87]
Gra/Pd	MOR	0.38 (mA cm^{-2}), 0.87 (mA mg^{-1})	4.22	[88]
Pd/rGO	MOR	22 (mA cm^{-2})	1.73	[89]
PtPd/rGO	MOR	252 (mA cm^{-2})	1.1	[89]
Pd-rGO	MOR	522 (mA mg^{-1})	6.05	[100]
PtIr PNWs/rGO	MOR	543 (mA mg^{-1})	1.09	[104]
RG-PdnD	MOR	0.509 (mA cm^{-2})	7.50	[106]
RG-PdnS	MOR	0.1274 (mA cm^{-2})	1.68	[106]
Pt-Co/G	MOR	12.3 (mA cm^{-2})	2.31	[114]
G-Au	MOR	0 (mA cm^{-2})	N/A	[119]
G-Pd	MOR	12.5 (mA cm^{-2})	2.78	[119]
G-AuPd@Pd	MOR	29 (mA cm^{-2})	2.76	[119]
Pt_3Pd_1/GO	MOR	7.07 (mA mg^{-1})	1.03	[120]
Pt_2Pd_1/GO	MOR	7.98 (mA mg^{-1})	1.11	[120]
Pt_1Pd_1/GO	MOR	14.4 (mA mg^{-1})	1.26	[120]
Pd/GNs	EOR	0.56 (mA cm^{-2})	4.00	[33]
Pd-Pt/GNs	EOR	7.69 (mA cm^{-2})	5.45	[33]
Pd/rGO	EOR	0.3 (mA m^{-2})	1.36	[27]
PdRu/rGO	EOR	0.52 (mA m^{-2})	1.44	[27]
PdSn/rGO	EOR	0.41 (mA m^{-2})	1.58	[27]
PdIr/rGO	EOR	0.19 (mA m^{-2})	0.95	[27]
PdNP/GNs	EOR	7.5 (mA cm^{-2})	0.95	[39]
PdPtNP/GNs	EOR	22.4 (mA cm^{-2})	1.83	[39]
Pd/rGO	EOR	22 (mA cm^{-2})	0.91	[76]
Ag/rGO	EOR	0 (mA cm^{-2})	N/A	[76]
Pd-Ag/rGO	EOR	90 (mA cm^{-2})	1.41	[76]
Pd/Cu/graphene	EOR	392.6 (mA mg^{-1})	2.98	[78]
PdNCs/G	EOR	429.847 (mA mg^{-1})	1.76	[79]
Pd/rGO	EOR	6.52 (mA cm^{-2})	0.815	[80]
PdAg/rGO	EOR	11.51 (mA cm^{-2})	1.24	[80]
Pd/rGO	EOR	897.56 (mA cm^{-2})	1.20	[84]
Pd-Au/rGO	EOR	2218.74 (mA cm^{-2})	1.03	[84]
Pd/rGO	EOR	835 (mA mg^{-1})	1.15	[85]
Pd-Ag/rGO	EOR	1601 (mA mg^{-1})	1.56	[85]
Pd-Cu/rGO	EOR	2105.4 (mA mg^{-1})	1.38	[86]
G-Pd	EOR	3.83 (mA cm^{-2})	1.17	[87]
Gra/Pd	EOR	1.48 (mA cm^{-2}), 3.35 (mA mg^{-1})	1.43	[88]
Pd/rGO	EOR	23 (mA cm^{-2})	0.602	[89]
PtPd/rGO	EOR	228 (mA cm^{-2})	0.92	[89]
PdPt@Pt/rGO	EOR	74.2 (mA mg^{-1})	0.780	[91]
PtPd/rGO	EOR	37.6 (mA mg^{-1})	1.19	[91]
Pd/rGO	EOR	13.7 (mA mg^{-1})	N/A	[91]

(*continued on next page*)

Table 4 (*continued*)

M/GNs catalyst	Type of oxidation	J_f (Anodic sweep)	I_f/I_b	Ref
PtPd NFs-rGO	EOR	52.31 (mA cm^{-2})	2.23	[92]
rGO-PD NPs	EOR	46.67 (mA cm^{-2})	0.94	[24]
Pd/GN1	FOR	210 (mA mg^{-1})	N/A	[32]
Pd/GN2	FOR	300 (mA mg^{-1})	N/A	[32]
Pd/rGO	FOR	308.4 (mA mg^{-1})	N/A	[81]
PdNi-NN/rGO	FOR	604.3 (mA mg^{-1})	N/A	[81]
Pd/rGO	FOR	3.21 (mA cm^{-2})	N/A	[82]
LDG/Pd	FOR	61.6 (mA cm^{-2})	N/A	[83]
rGO/Pd	FOR	34.6 (mA cm^{-2})	N/A	[83]
AP-Pd/GN	FOR	466.3 (mA mg^{-1})	N/A	[102]
Pd/GN	FOR	213 (mA mg^{-1})	N/A	[102]
Pd/GNP	FOR	13.78 (mA cm^{-2}), 3990 (mA mg^{-1})	N/A	[113]
FS-Pd/GO	GOR	56 (μA mg^{-1})	N/A	[105]
Au/rGO	GOR	7.4 (mA cm^{-2})	N/A	[111]
Au/Ag/rGO	GOR	16.2 (mA cm^{-2})	N/A	[111]
Ag/Au/rGO	GOR	15.2 (mA cm^{-2})	N/A	[111]

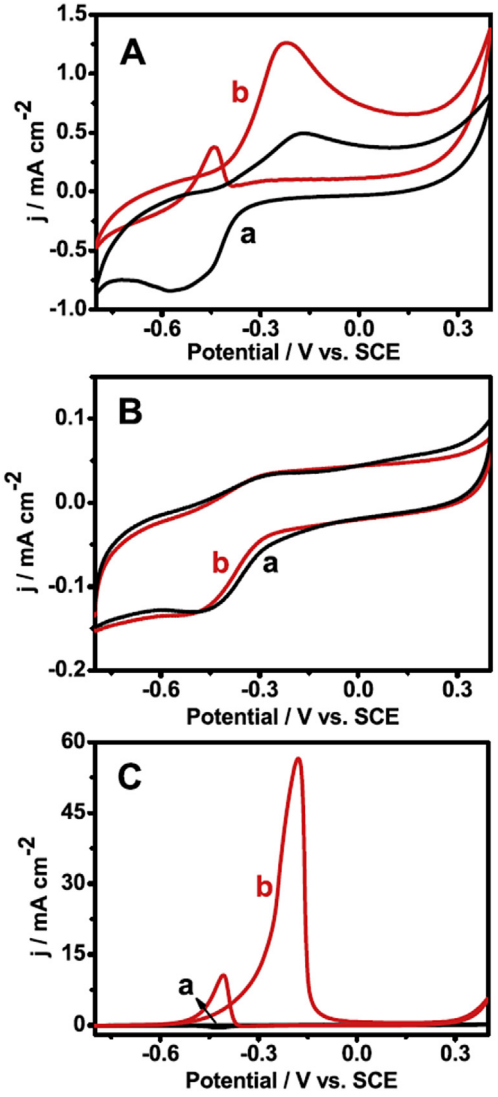

Fig. 3. CVs of (a) Pd-Cu NC/RGOs, (b) RGOs, and (c) Pd black modified electrodes without (curve a) and with (curve b) 3.0 M methanol in 1.0 M KOH at the scanning rate of 50 mV s^{-1} (reproduced with permission from Elsevier B.V. [90]).

KOH solution, when compared with the Pd black. This is because no methanol oxidation peak or weak peak was observed in both the Pd-Cu NC/rGOs and rGOs system, while the Pd black one was very strong [90]. Recently, semiconductor electrocatalyst like MO_x/GNs [121] and metal-free foreign element doped GNs or 3D rGO (B, N mono-doped GNs, BN co-doped GNs, and B-doped 3D rGO) [137,138,140,142,146,148] have drawn strong attention to the ORR reactions in fuel cell reaction. Similar to the EOR and MOR catalyzed by M/GNs or M/GA, CV scan is the general methodology on the ORR behavior analysis. The results from different analysis reflected that the oxygen reduction ability contributed from such materials was very strong [121,137,138,140,142,146,148]. This is reflected in the enhancement of the cathodic swap peak current density (1.2–3.8 mA cm^{-2}) [140,146] when compared to commercial Pt/C (1.5 mA cm^{-2}) [146], or more positive onset potential (0.8–1 V vs RHE) [121,140,142] relative to the bare rGO, MO_x, or Pt based catalyst. The results of Zhou et al. [146] reflected that the oxygen reduction ability, contributed from B-doped 3D rGO, reduced by different boron containing reducing agents, was comparable to that of commercial Pt/C catalyst. They also showed that much stronger selectivity in ORR upon addition of methanol, and higher durability than the commercial Pt/C in prolonged ORR cycles (2500 cycles) [146].

3.2. Supercapacitor

MO_x/GNs [125,126,135] and metal free doped GNs [141,150] played an important role in supercapacitor research, which are listed in Table 5. The measured specific capacitance of MO_x/GNs was about 2–3 times larger than that of the corresponding bare MO_x (~60–135 F g^{-1}) and GNs (72.2–157 F g^{-1}), with values in the range of 95–308 F g^{-1} [125,126,135]. Similar tendency was also recorded in the single foreign element doped GNs [141,150]. Dou et al. [150] observed that the performance of GNs was enhanced when it was doped with two foreign elements compared to both bare GNs (77 F g^{-1}) or single element doped GNs (B/GNs: 83 F g^{-1}, N/GNs: 111 F g^{-1}), but the overall value was not very high, just about 131 F g^{-1}. It showed strong stability as the capacitance retention was lower than 10% over 1500 cycles scanning [150]. It should be noted that such results may be case dependent for different research groups with different electrolytes [141,150]. For example, the capacitance of B/GNs recorded by Dou's group (83 F g^{-1}, 1 M H_2SO_4) [150] was smaller than that recorded by Yeom's group (448 F g^{-1}, 6 M KOH) [141] when the type and concentration of electrolyte used in these system were different. Besides the use of loaded GNs, pure GNs on secondary substrate such as NF was also the target of research carried out by different groups, and large capacitances in the range of 236 F g^{-1} to 334 F g^{-1} were obtained [37,38,40]. The retardation in capacitance among these samples was also slow through 1000 cycles [37,38] to 10,000 cycles

Table 5
List of the 2D graphene and 3D graphene based supercapacitor materials.

2D graphene based supercapacitor materials	References	3D graphene based supercapacitor materials	Ref
ZnO/GNs	[125,126,135]	Co/GA	[108]
Gr/SnO_2	[127]	MnO_2/GF	[61]
BCN/GNs	[150]	GA/TiO_2	[128]
N/GNs	[150]	B-doped GA	[143]
B/GNs	[141,150]	N-doped GH	[144]
3D-NiGO	[37]	N-doped GA	[143,145]
HrGO/NF	[38]	BN co-doped GA	[143]
3D RGO/Ni foam	[40]	NG/NF	[147]
		Pure GH	[19,25,45,46,51,54,63]
		Pure GA	[19,20,25,45,49,53,128]
		rGO@Ni foam	[152]

[40] of operation. Besides the 2D graphene based materials, M/GA [108], MO_x/GF and MO_x/GA [61,128], foreign elements doped GH or GA [143–145], and pure GH or GA [19,20,25,45,46,49,51,54,63,128], were also used as capacitor materials, as illustrated in Table 5. The activity of MO_x/GF, or doped GA or GH was comparable, or even higher than that of 2D MO_x/GNs and foreign element doped GNs as mentioned in previous section (95–308 F g^{-1}), which is reflected from the value range of 67–670 F g^{-1} under various scanning rates in the capacitance analysis [61,143–145]. Some research groups also attempted to use M/GA in the supercapacitor research such as Co/GA. The result from Bao et al. [108] showed that the capacitance of Co/GA was comparable to the traditional materials used in the supercapacitor, with a specific capacity of 387 F g^{-1} in acidic solution. Even though some of them were bare GH or GA, the performance (100–331.3 F g^{-1}) was also higher than those 2D GNs based capacitors.

In common practice, the GH or GA was cut into thin disc before use [25,45,46,49,51,54,61,63,143–145]. Recently, some research groups developed a binder free technique for the supercapacitor electrode preparation that can reduce the cost of electrode production, increase the rate capability of the double layer capacitor electrodes, and enhance the ion diffusion in the capacitor [19,20]. Meanwhile, NF was developed as a new template for the GA capacitor electrode preparation. The recorded specific capacitance of the pure GA/NF and GH/NF, and N-doped GA/NF (NG/NF) synthesized, was 366 F g^{-1} (41.1–45.6 mF cm^{-2}) (Fig. 4), and 223–442 F g^{-1}, respectively with stable performance during 1600–3000 cycles operations which were comparable to the bulk of pure GA or GH, and the N-doped graphene based materials as mentioned above and in previous sections [19,20,53,147,152]. Such results provided the possibility of a convenient and high performance capacitor electrode production with low cost in industrial manner in the future.

Till date, KOH and NaOH solution are commonly used electrolyte in the graphene based supercapacitor investigation. Special electrolyte like saline water was also tried in capacitor research. For example, El-Deen's group found that Gr/SnO_2 exhibited strong specific capacitance with a value of 323 F g^{-1} in 1 M NaCl solution, with stable performance over 50 cycles of operation [127]. The Gr/SnO_2 showed strong salt removal ability with a maximum removal percentage of 83%, which was higher than that of using pristine graphene (Gr, ~65%). On the other hand, Yin et al. [128] observed that the GA/TiO_2 exhibited extremely strong specific current (~16 A g^{-1}), and specific capacitance (120 F g^{-1}) in saline water (0.1 M NaCl), which were much higher than commercial activated carbon. The capacitance can be kept at a constant level in prolong scanning with the use of NaCl solution (1000 cycles). The GA/TiO_2 also exhibited strong desalination ability in 0.1 M NaCl solution. The study by Yi et al. [128] revealed the potential for fresh water production through desalination using graphene based capacitor materials in the future [127,128].

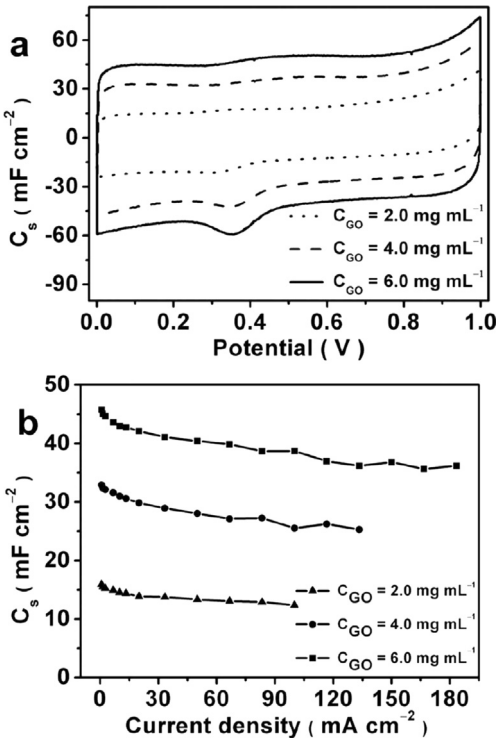

Fig. 4. (a) CV curves of the G-Gel/NF ECs prepared by reducing GO dispersions with different concentrations; scan rate = 50 mV s^{-1}. (b) Plots of C_s of G-Gel/NF ECs versus current density. (reproduced with permission from WILEY-VCH Verlag GmbH & Co. [19]).

3.3. Lithium-ion battery

The use of GNs based materials in Li-ion battery is another focus in recent years, of which MO_x/GNs and B-doped GNs were commonly used materials [13,122,124,131,132,149]. Observation from different groups showed that the charging and discharging capacity ranged between 88 and 430 mAh g^{-1} for the ZnO/GNs and TiO_2/GNs under different current density settings [122,124,131,132], while that of B-GNs and N-GNs were ranged between 139 and 350 mAh g^{-1} or 0.05 mAh cm^{-2} [13,149]. One of the examples indicated that the stability of the B-GNs was strong over 20–50 cycles of service, as the corresponding charging and discharging capacity varied a little after full activation [149]. The performance was around two times stronger than that of bare carbon paper,

graphene, or corresponding bare metal oxides, which was due to 1) the induction of the defect on the GNs or 2) reduction of the hostility of the electrode through the N or B doping to GNs network [13,149], or 3) due to the improvement of the conductivity of MO_x after loading to the GNs network [122,124,131,132].

3.4. Photocurrent generation via solar cell and water splitting reaction

In the solar cell research, dye sensitized solar cell (DSSC) was one of most popularly studied solar cells in the past three decades due to their high conversion efficiency (12%) and low cost [130]. Recently, TiO_2/GNs and Pt/rGO based materials have been used in DSSC research [115,130]. In the study of counter electrode, Chen et al. [115] reported that Pt/rGO exhibited very strong activity compared to the Pt counter electrode and rGO counter electrodes, reflected by the high short circuit current density (11.6 mA cm^{-2}) and open circuit voltage (0.78 V). Shu et al. [130] found that the TiO_2/GNs photoanode-driven DSSC performed better than the P25 photoanode, as reflected by the high short circuit current density (12.2 mA cm^{-2}), with an open circuit voltage of 0.67 V, and conversion efficiency of 5.5% when compared to the one of P25. There were variations in the conversion efficiency for P25/rGO, which were found not to be related to the increase in the P25 loading [130]. The working principle and the corresponding performance was shown in Fig. 5 [130].

Besides the use of 2D GNs as the DSSC materials, 3D graphene prepared from CVD on NF was an alternative choice in recent years, due to the enhanced electrical conductivity compared with the bare P25 and 2D GNs and chemically derived graphene (CDG) [58]. Tang et al. [58] developed the 3D graphene based DSSC, composed of a photoanode (P25/3DGN) and a counter electrode (3DGN). Results shown in Fig. 6 revealed that the short circuit current density and efficiency of the DSSC were clearly enhanced, compared to the pure P25 or CDG driven DSSC. When the 3DGN loading in the P25/3DGN photoanode was increased, the DSSC performance was also increased due to the increase in the electron transport channels. However, further increase in the 3DGN loading resulted in a reduction of the cell performance due to the heat generation caused by the excessive photon absorption by the black 3DGN [58]. Based on the above mentioned result, they further built the DSSC with the scheme shown in Fig. 7, which showed a strong efficiency up to 5.9%, when the thin 3DGN based electrode was used [58].

Other than the applications for DSSC, 2D GNs based materials have also adopted for hydrogen production. The process involves hydrogen generation from water splitting in either pure water or methanol/water binary solution. The results from Gao's group on H_2 production through water splitting showed that not only did the catalyst induced high rate of hydrogen production (305.6 μmol h^{-1}), but that the photocurrent produced from such reaction (32 μA cm^{-2}) was also higher than that of the bare TiO_2 (10 μA cm^{-2}) [129].

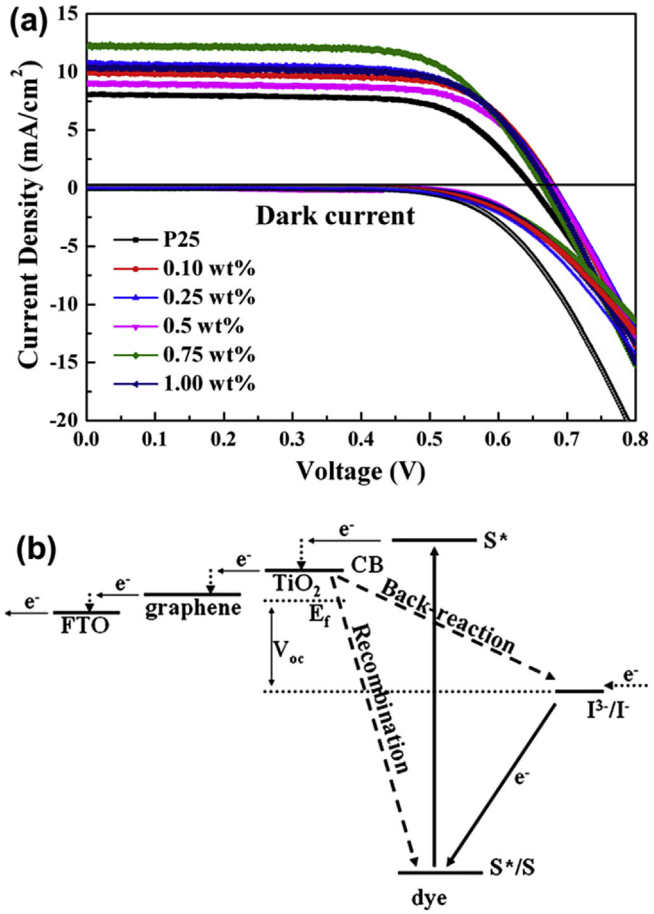

Fig. 5. (a) J-V curves of DSSCs of various RGO-P25 composites films and (b) work principle of DSSCs based on various RGO-P25 composite films (reproduced with permission from Elsevier B.V. [130]).

4. Challenges on the use of graphene based materials in green energy device research

Till to date, most of works on the use of 2D and 3D graphene as electrode materials was still stayed in the traditional framework of mind. Most of the production methods were destructive and caused wastage in nature, such as the use of ultrasonic method for the electrode fabrication with the use of stabilizer or conductive binder to hold the composite on the secondary electrode. However, the risk of 3D porous structures destruction by ultrasound will highly increase, which will make them no difference from the 2D graphene based materials. In addition, the use of binder also have the risk of active surface area reduction, which may result in performance reduction and extra wastage of chemicals in the fabrication process. This is especially obvious in the electrochemical electrode preparation. The use of non-destructive binder-free fabrication method through the direct growth of 2D or 3D graphene on the electrode substrate can eliminate this problem [19,20,30]. However, this method was seldom used compared with the traditional fabrication methods which were still used widely [19,20,30,37,38,40,53,147,152]. Nevertheless, this kind of method provided an alternative solution for clean electrode fabrication, which may be a potentially low cost production pathway in future research of green energy production. In addition, the research in glucose electrooxidation is relatively fewer in number relative to the extensive works in the MOR and EOR studies [105,111]. Extra attention needs to be paid due to the strong reactivity of the graphene based products in the anodic reaction, and the high abundance of glucose from the food waste as a potential fuel for energy generation.

Relative to the solar cell electrode study, the use of graphene based materials in the photocurrent production via water splitting is still lacking [129]. This provides room for further research in systematic manner in future based on the excellent activity of semiconductor loaded graphene in the DSSC studies [58].

5. Conclusions and outlook

A large amount of research has been conducted in the

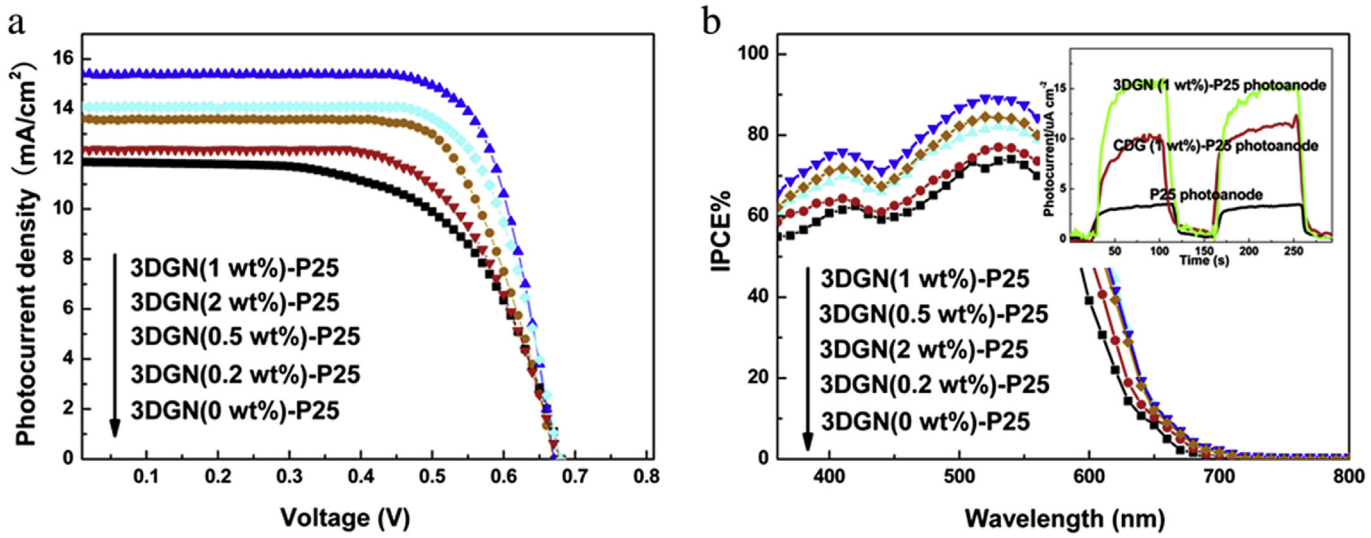

Fig. 6. (a) J-V curves and (b) IPCE curves of the DSSCs with different photoanodes, the inset shows photocurrent of the pure P25, CDG (1-wt%)-P25 and 3DGN (1-wt%)-P25 photoanodes (reproduced with permission from Elsevier B.V. [58]).

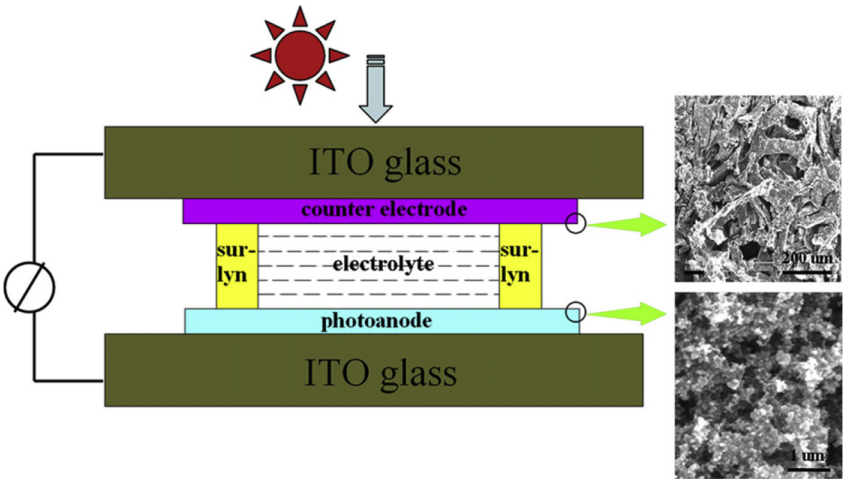

Fig. 7. Schematic image of the DSSC with 3DGN based photoanode and counter electrode, and the SEM images of the electrodes are displayed (reproduced with permission from Elsevier B.V. [58]).

development of 2D and 3D structured graphene based materials with special attention on green synthesis, and their applications. The results from green energy production showed strong activity exhibited by various graphene products. However, the challenges in graphene development in such area still exist. First, even though green energy research of graphene based materials has continued over the past decade, 2D structured graphene is still the major focus. The techniques involved are still at the fundamental level, such as the multiple step electrodes preparation in chemical cell researches and half-cell reaction oriented research, and the use of binders for the 2D graphene based electrocatalyst preparation. Secondly, except for the matured pathway through CVD, the use of bulk GA or GH was extensively reported. These involved the destructive fabrication technique in real applications, such as the use of ultrasonic dispersion, and the use of stabilizer or conductive binders for the electrode fabrication. This method will make the electrode preparation very complicated and may increase wastage due to the use of extra chemicals throughout the process. Performance of GA or GH based materials may be reduced due to the 3D structure destruction and masking of active surface area. Non-destructive fabrication or growth technique for the GA or GH hybrid composite then becomes important, as the porous substrate can fit tightly with the porous 3D GA or GH, which enhances the electrical conductivity and increases the active surface area of the GA or GH. This is very important for the use of GA as direct electrodes in supercapacitor, fuel cell, lithium battery, or dye-sensitized solar cell. More importantly, it may be beneficial to widen the area of research and applications in green energy production. However, the study, regarding non-destructive fabrication technique, of GA or GH to the secondary substrate or one-step growth of GH or GA on the secondary substrate was relatively few in number when compared to huge number of report on the destructive fabrication techniques. Besides the materials preparation, the breakthrough on the application of graphene based materials is still not obvious. Only very few number of works on the alternative applications were spinned off from the traditional research, such as the desalination of water for exploring new kind of fresh water supply through capacitor operation. The studies on the photocurrent production via water splitting are also lacking. In order to create a promising future for graphene based materials, especially the 3D

graphene materials for real applications, advanced studies in fuel-cell, and water splitting have become a prospective area of research.

Acknowledgement

This project is supported by the URC's PDF scheme and the CRCG grant # 201511159115 of the University of Hong Kong.

Abbreviation list

CVD	Chemical vapor deposition
2D	Two dimensional
3D	Three dimensional
GNs	Graphene nanosheets
AP-Pd/GN	As-prepared Pd loaded graphene nanosheets
LDG	Low defeat graphene
H_2O_2	Hydrogen peroxide
VC	Vitamin C or L-ascorbic acid
DI	Deionized water
EG	Ethylene glycerol
PD	Propane-1, 2-diol
EDA	Ethylenediamine
CCG	Chemically converted graphene
TBOT	Titanium *n*-butoxide
TBT	Terbutyl titanate, tetra-*n*-butyl titanate
$ScCO_2$	Supercritical carbon dioxide
THF	Tetrahydrofuran
OH·	Hydroxyl radical
MOR	Methanol oxidation reaction
EOR	Ethanol oxidation reaction
FOR	Formic acid oxidation reaction
GOR	Glucose oxidation reaction
ORR	Oxygen reduction reaction
BCN graphene	Boron nitrogen codoped graphene
GH	Graphene hydrogel
GA	Graphene aerogel
GF	Graphene foam
GP	Graphite paper
GOF	Graphene oxide foam
3DGN	Three dimensional graphene nanosheets
CNT	Carbon nanotubes
MO_x	Metal oxides
AC	Alternative current
GC	Glassy carbon electrode

References

[1] M.J. Allen, V.C. Tung, R.B. Kaner, Chem. Rev. 110 (2010) 132–145.
[2] C.N.R. Rao, A.K. Sood, K.S. Subrahmanyam, A. Govindaraj, Angew. Chem. Int. Ed. 48 (2009) 7752–7777.
[3] Y. Zhu, S. Murali, W. Cai, X. Li, J.W. Suk, J.R. Potts, R.S. Ruoff, Adv. Mater 22 (2010) 3906–3924.
[4] K.I. Bolotin, K.J. Sikes, Z. Jiang, M. Klima, G. Fudenberg, J. Hone, P. Kim, H.L. Stormer, Solid State Commun. 146 (2008) 351–355.
[5] M.D. Stoller, S. Park, Y. Zhu, J. An, R.S. Ruoff, Nano Lett. 8 (2008) 3498–3502.
[6] C. Lee, X. Wei, J.W. Kysar, J. Hone, Science 321 (2008) 385–388.
[7] A.A. Balandin, S. Ghosh, W. Bao, I. Calizo, D. Teweldebrhan, F. Miao, C.N. Lau, Nano Lett. 8 (2008) 902–907.
[8] R.R. Nair, P. Blake, A.N. Grigorenko, K.S. Novoselov, T.J. Booth, T. Stauber, N.M.R. Peres, A.K. Geim, Science 320 (2008), 1308–1308.
[9] F. Perreault, A.F. de Faria, M. Elimelech, Chem. Soc. Rev. 44 (2015) 5861–5896.
[10] N. Zhang, M.Q. Yang, S.Q. Liu, Y.G. Sun, Y.J. Xu, Chem. Rev. 115 (2015) 10307–10377.
[11] S. Mao, G.H. Lu, J.H. Chen, Nanoscale 7 (2015) 6924–6943.
[12] N. Shang, P. Papakonstantinou, P. Wang, S. Ravi, P. Silva, J. Phys. Chem. C 114 (2010) 15837–15841.
[13] A.L.M. Reddy, A. Srivastava, S.R. Gowda, H. Gullapalli, M. Dubey, P.M. Ajayan, ACS Nano 4 (2010) 6337–6342.
[14] W.S. Hummers, R.E. Offeman, J. Am. Chem. Soc. 80 (1958) 1339.
[15] N.I. Kovtyukhova, P.J. Ollivier, B.R. Martin, T.E. Mallouk, S.A. Chizhik, E.V. Buzaneva, A.D. Gorchinskiy, Chem. Mater. 11 (1999) 771–778.
[16] Z. Sui, X. Zhang, Y. Lei, Y. Luo, Carbon 49 (2011) 4314–4321.
[17] L. Zhang, N. Li, H. Jiu, G. Qi, Y. Huang, Ceram. Int. 41 (2015) 6256–6262.
[18] P. Wang, J. Wang, X. Wang, H. Yu, J. Yu, M. Lei, Y. Wang, Appl. Catal. B-Environ. 132–133 (2013) 452–459.
[19] J. Chen, K.X. Sheng, P.H. Luo, C. Li, G.Q. Shi, Adv. Mater 24 (2012) 4569–4573.
[20] S.B. Ye, J.C. Feng, P.Y. Wu, ACS Appl. Mater. Interfaces 5 (2013) 7122–7129.
[21] P.-Q. Wang, Y. Bai, P.-Y. Luo, J.-Y. Liu, Catal. Commun. 38 (2013) 82–85.
[22] S. Morales-Torres, L.M. Pastrana-Martinez, J.L. Figueiredo, J.L. Faria, A.M.T. Silva, Appl. Surf. Sci. 275 (2013) 361–368.
[23] W. Sun, X. Lu, Y. Tong, Z. Zhang, J. Lei, G. Nie, C. Wang, Int. J. Hydrogen Energy 39 (2014) 9080–9086.
[24] D.H. Nagaraju, G.S. Suresh, ECS Electrochem. Lett. 1 (2012) F21–F23.
[25] X. Zhang, Z. Sui, B. Xu, S. Yue, Y. Luo, W. Zhan, B. Liu, J. Mater. Chem. 21 (2011) 6494–6497.
[26] Y. Kim, Y. Noh, E.J. Lim, S. Lee, S.M. Choi, W.B. Kim, J. Mater. Chem. A 2 (2014) 6976–6986.
[27] E.J. Lim, Y. Kim, S.M. Choi, S. Lee, Y. Noh, W.B. Kim, J. Mater. Chem. A 3 (2015) 5491–5500.
[28] S.H. Kim, G.H. Jeong, D. Choi, S. Yoon, H.B. Jeon, S.M. Lee, S.W. Kim, J. Colloid Interf. Sci. 389 (2013) 85–90.
[29] X. Chen, B. Su, G. Wu, C.J. Yang, Z. Zhuang, X. Wang, X. Chen, J. Mater. Chem. 22 (2012) 11284–11289.
[30] C.-H.A. Tsang, K.N. Hui, K.S. Hui, L. Ren, J. Mater. Chem. A 2 (2014) 17986–17993.
[31] M. Sawangphruk, A. Krittayavathananon, N. Chinwipas, J. Mater. Chem. A 1 (2013) 1030–1034.
[32] J. Yang, C. Tian, L. Wang, H. Fu, J. Mater. Chem. 21 (2011) 3384–3390.
[33] X. Yang, Q.D. Yang, J. Xu, C.S. Lee, J. Mater. Chem. 22 (2012) 8057–8062.
[34] J.L. Zhang, H.J. Yang, G.X. Shen, P. Cheng, J.Y. Zhang, S.W. Guo, Chem. Commun. 46 (2010) 1112–1114.
[35] M. Khan, A. Bin Yousaf, M. Chen, C. Wei, X. Wu, N. Huang, Z. Qi, L. Li, J. Power Sources 282 (2015) 520–528.
[36] R. Awasthi, R.N. Singh, Carbon 51 (2013) 282–289.
[37] C.L. Zheng, J.L. Zhang, Q. Zhang, B. You, G.L. Chen, Electrochim. Acta 152 (2015) 216–221.
[38] Y.B. Xie, Y.Y. Zhan, J. Porous Mater. 22 (2015) 403–412.
[39] X.M. Chen, Z.X. Cai, X. Chen, M. Oyama, J. Mater. Chem. A 2 (2014) 315–320.
[40] J. Yang, E.W. Zhang, X.F. Li, Y.H. Yu, J. Qu, Z.Z. Yu, ACS Appl. Mater. Interfaces 8 (2016) 2297–2305.
[41] S. Eigler, M. Enzelberger-Heim, S. Grimm, P. Hofmann, W. Kroener, A. Geworski, C. Dotzer, M. Rockert, J. Xiao, C. Papp, O. Lytken, H.P. Steinruck, P. Muller, A. Hirsch, Adv. Mater 25 (2013) 3583–3587.
[42] S. Eigler, C. Dotzer, A. Hirsch, M. Enzelberger, P. Muller, Chem. Mater. 24 (2012) 1276–1282.
[43] S. Kim, S. Zhou, Y.K. Hu, M. Acik, Y.J. Chabal, C. Berger, W. de Heer, A. Bongiorno, E. Riedo, Nat. Mater. 11 (2012) 544–549.
[44] S. Eigler, C. Dotzer, A. Hirsch, Carbon 50 (2012) 3666–3673.
[45] V.H. Luan, H.N. Tien, L.T. Hoa, N.T.M. Hien, E.-S. Oh, J. Chung, E.J. Kim, W.M. Choi, B.-S. Kong, S.H. Hur, J. Mater. Chem. A 1 (2013) 208–211.
[46] L. Zhang, G. Shi, J. Phys. Chem. C 115 (2011) 17206–17212.
[47] H. Hu, Z. Zhao, W. Wan, Y. Gogotsi, J. Qiu, Adv. Mater 25 (2013) 2219–2223.
[48] Z. Xu, Y. Zhang, P. Li, C. Gao, ACS Nano 6 (2012) 7103–7113.
[49] W. Si, X. Wu, J. Zhou, F. Guo, S. Zhou, H. Chu, W. Xing, Nanoscale Res. Lett. 8 (2013) 247.
[50] M.A. Worsley, P.J. Pauzauskie, T.Y. Olson, J. Biener, J.H. Satcher Jr., T.F. Baumann, J. Am. Chem. Soc. 132 (2010) 14067–14069.
[51] K.-x. Sheng, Y.-x. Xu, C. Li, G.-q. Shi, New Carbon Mater 26 (2011) 9–15.
[52] B. Adhikari, A. Biswas, A. Banerjee, ACS Appl. Mater. Interfaces 4 (2012) 5472–5482.
[53] J.H. Chang, Y.H. Hung, X.F. Luo, C.H. Huang, S.M. Jung, J.K. Chang, J. Kong, C.Y. Su, RSC Adv. 6 (2016) 8384–8394.
[54] Y. Xu, K. Sheng, C. Li, G. Shi, ACS Nano 4 (2010) 4324–4330.
[55] J. Li, J. Li, H. Meng, S. Xie, B. Zhang, L. Li, H. Ma, J. Zhang, M. Yu, J. Mater. Chem. A 2 (2014) 2934–2941.
[56] H.N. Lim, N.M. Huang, S.S. Lim, I. Harrison, C.H. Chia, Int. J. Nanomed. 6 (2011) 1817–1823.
[57] X. Song, L. Lin, M. Rong, Y. Wang, Z. Xie, X. Chen, Carbon 80 (2014) 174–182.
[58] B. Tang, G. Hu, H. Gao, Z. Shi, J. Power Sources 234 (2013) 60–68.
[59] T. Maiyalagan, X.C. Dong, P. Chen, X. Wang, J. Mater. Chem. 22 (2012) 5286–5290.
[60] C.C. Kung, P.Y. Lin, Y.H. Xue, R. Akolkar, L.M. Dai, X. Yu, C.C. Liu, J. Power Sources 256 (2014) 329–335.
[61] U.M. Patil, J.S. Sohn, S.B. Kulkarni, H.G. Park, Y. Jung, K.V. Gurav, J.H. Kim, S.C. Jun, Mater. Lett. 119 (2014) 135–139.
[62] S. Yang, L. Chen, L. Mu, P.-C. Ma, J. Colloid Interf. Sci. 430 (2014) 337–344.
[63] M. Yu, Y. Huang, C. Li, Y. Zeng, W. Wang, Y. Li, P. Fang, X. Lu, Y. Tong, Adv. Funct. Mater. 25 (2015) 324–330.
[64] H. Zhao, X. Song, H. Zeng, e168, NPG Asia Mater. 7 (2015).
[65] J.-X. Feng, Q.-L. Zhang, A.-J. Wang, J. Wei, J.-R. Chen, J.-J. Feng, Electrochim. Acta 142 (2014) 343–350.
[66] K. Wu, Q. Zhang, D. Sun, X. Zhu, Y. Chen, T. Lu, Y. Tang, Int. J. Hydrogen Energy 40 (2015) 6530–6537.
[67] N. Li, S. Tang, X. Meng, J. Mater. Sci. Technol. 30 (2014) 1071–1077.

[68] S.-S. Li, J. Yu, Y.-Y. Hu, A.-J. Wang, J.-R. Chen, J.-J. Feng, J. Power Sources 254 (2014) 119–125.
[69] Y. Zhang, G. Chang, H. Shu, M. Oyama, X. Liu, Y. He, J. Power Sources 262 (2014) 279–285.
[70] L.-R. Zhang, J. Zhao, M. Li, H.-T. Ni, J.-L. Zhang, X.-M. Feng, Y.-W. Ma, Q.-L. Fan, X.-Z. Wang, Z. Hu, W. Huang, New J. Chem. 36 (2012) 1108–1113.
[71] C.-S. Liao, C.-T. Liao, C.-Y. Tso, H.-J. Shy, Mater. Chem. Phys. 130 (2011) 270–274.
[72] J.-D. Qiu, G.-C. Wang, R.-P. Liang, X.-H. Xia, H.-W. Yu, J. Phys. Chem. C 115 (2011) 15639–15645.
[73] Y. Li, W. Gao, L. Ci, C. Wang, P.M. Ajayan, Carbon 48 (2010) 1124–1130.
[74] J. Zang, Y. Wang, L. Bian, J. Zhang, F. Meng, Y. Zhao, R. Lu, X. Qu, S. Ren, Carbon 50 (2012) 3032–3038.
[75] H. Huang, H. Chen, D. Sun, X. Wang, J. Power Sources 204 (2012) 46–52.
[76] J. Liu, H. Zhou, Q. Wang, F. Zeng, Y. Kuang, J. Mater. Sci. 47 (2012) 2188–2194.
[77] Y. Li, L. Tang, J. Li, Electrochem. Commun. 11 (2009) 846–849.
[78] Q. Dong, Y. Zhao, X. Han, Y. Wang, M. Liu, Y. Li, Int. J. Hydrogen Energy 39 (2014) 14669–14679.
[79] Y. Zhang, Q. Huang, G. Chang, Z. Zhang, T. Xia, H. Shu, Y. He, J. Power Sources 280 (2015) 422–429.
[80] C. Peng, M. Liu, Y. Hu, W. Yang, J. Guo, Y. Zheng, RSC Adv. 5 (2015) 49899–49903.
[81] D. Bin, B. Yang, F. Ren, K. Zhang, P. Yang, Y. Du, J. Mater. Chem. A 3 (2015) 14001–14006.
[82] S. Yang, J. Dong, Z. Yao, C. Shen, X. Shi, Y. Tian, S. Lin, X. Zhang, Sci. Rep. 4 (2014) 4501.
[83] H.J. Huang, X. Wang, J. Mater. Chem. 22 (2012) 22533–22541.
[84] F. Li, Y. Guo, R. Li, F. Wu, Y. Liu, X. Sun, C. Li, W. Wang, J. Gao, J. Mater. Chem. A 1 (2013) 6579–6587.
[85] L. Li, M. Chen, G. Huang, N. Yang, L. Zhang, H. Wang, Y. Liu, W. Wang, J. Gao, J. Power Sources 263 (2014) 13–21.
[86] H. Na, L. Zhang, H. Qiu, T. Wu, M. Chen, N. Yang, L. Li, F. Xing, J. Gao, J. Power Sources 288 (2015) 160–167.
[87] L. Gao, W. Yue, S. Tao, L. Fan, Langmuir 29 (2013) 957–964.
[88] D.H. Nagaraju, S. Devaraj, P. Balaya, Mater. Res. Bull. 60 (2014) 150–157.
[89] S.-S. Li, J.-N. Zheng, X. Ma, Y.-Y. Hu, A.-J. Wang, J.-R. Chen, J.-J. Feng, Nanoscale 6 (2014) 5708–5713.
[90] J.-J. Lv, S.-S. Li, A.-J. Wang, L.-P. Mei, J.-J. Feng, J.-R. Chen, Z. Chen, J. Power Sources 269 (2014) 104–110.
[91] S.-S. Li, J.-J. Lv, L.-N. Teng, A.-J. Wang, J.-R. Chen, J.-J. Feng, ACS Appl. Mater. Interfaces 6 (2014) 10549–10555.
[92] J.-J. Lv, N. Wisitruangsakul, J.-J. Feng, J. Luo, K.-M. Fang, A.-J. Wang, Electrochim. Acta 160 (2015) 100–107.
[93] H.S. Chen, Y.T. Liang, T.Y. Chen, Y.C. Tseng, C.W. Liu, S.R. Chung, C.T. Hsieh, C.E. Lee, K.W. Wang, Chem. Commun. 50 (2014) 11165–11168.
[94] C.-C. Huang, N.-W. Pu, C.-A. Wang, J.-C. Huang, Y. Sung, M.-D. Ger, Sep. Pur. Technol. 82 (2011) 210–215.
[95] H. Wu, D. Wexler, H. Liu, J. Solid State Electrochem. 15 (2011) 1057–1062.
[96] Y. Shao, S. Zhang, C. Wang, Z. Nie, J. Liu, Y. Wang, Y. Lin, J. Power Sources 195 (2010) 4600–4605.
[97] L. Ren, K.S. Hui, K.N. Hui, J. Mater. Chem. A 1 (2013) 5689–5694.
[98] J. Li, C.-y. Liu, Y. Liu, J. Mater. Chem. 22 (2012) 8426–8430.
[99] M. Liu, C. Peng, W. Yang, J. Guo, Y. Zheng, P. Chen, T. Huang, J. Xua, Electrochim. Acta 178 (2015) 838–846.
[100] Y. Wang, Y. Zhao, W.T. He, J. Yin, Y.Q. Su, Thin Solid Films 544 (2013) 88–92.
[101] S. Chen, J.W. Zhu, L. Qiu, D. Li, X. Wang, Chem. Eur. J. 19 (2013) 7631–7636.
[102] H. Zhao, J. Yang, L. Wang, C. Tian, B. Jiang, H. Fu, Chem. Commun. 47 (2011) 2014–2016.
[103] S. Sun, G. Zhang, N. Gauquelin, N. Chen, J. Zhou, S. Yang, W. Chen, X. Meng, D. Geng, M.N. Banis, R. Li, S. Ye, S. Knights, G.A. Botton, T.-K. Sham, X. Sun, Sci. Rep. 3 (2013) 1775.
[104] L. Hong, Y. Hao, Y. Yang, J. Yuan, L. Niu, Nanotechnol 26 (2015) 045604.
[105] Q. Wang, X. Cui, W. Guan, W. Zheng, J. Chen, X. Zheng, X. Zhang, C. Liu, T. Xue, H. Wang, Z. Jin, H. Teng, J. Phys. Chem. Solids 74 (2013) 1470–1474.
[106] S.C. Sahu, A.K. Samantara, A. Dash, R.R. Juluri, R.K. Sahu, B.K. Mishra, B.K. Jena, Nano Res. 6 (2013) 635–643.
[107] M. Wojnicki, M. Luty-Błocho, I. Dobosz, J. Grzonka, K. Pacławski, K.J. Kurzydłowski, K. Fitzner, Mater. Sci. Appl. 4 (2013) 162–169.
[108] Q. Bao, K.N. Hui, K.S. Hui, Y. Wang, X. Hong, Mater. Res. Bull. 56 (2014) 92–97.
[109] S. Yun, S. Lee, C. Shin, S. Park, S.J. Kwon, H.S. Park, Electrochim. Acta 180 (2015) 902–908.
[110] R. Wang, Z. Wu, C. Chen, Z. Qin, H. Zhu, G. Wang, H. Wang, C. Wu, W. Dong, W. Fan, J. Wang, Chem. Commun. 49 (2013) 8250–8252.
[111] Q. Shi, G. Diao, S. Mu, Electrochim. Acta 133 (2014) 335–346.
[112] M. Rajkumar, B. Devadas, S.-M. Chen, P.-C. Yeh, Colloids Surf. Physicochem. Eng. Asp. 452 (2014) 39–45.
[113] Q.-S. Chen, Z.-N. Xu, S.-Y. Peng, Y.-M. Chen, D.-M. Lv, Z.-Q. Wang, J. Sun, G.-C. Guo, J. Power Sources 282 (2015) 471–478.
[114] R. Ojani, J.-B. Raoof, M.G. Li, R. Valiollahi, J. Power Sources 264 (2014) 76–82.
[115] C. Chen, M. Long, H. Wu, W. Cai, Sci. China-Chem. 56 (2013) 354–361.
[116] S. Liu, J. Wang, J. Zeng, J. Ou, Z. Li, X. Liu, S. Yang, J. Power Sources 195 (2010) 4628–4633.
[117] Y.-G. Zhou, J.-J. Chen, F.-b. Wang, Z.-H. Sheng, X.-H. Xia, Chem. Commun. 46 (2010) 5951–5953.
[118] K.S. Hui, K.N. Hui, D.A. Dinh, C.H. Tsang, Y.R. Cho, W. Zhou, X.T. Hong, H.H. Chun, Acta Mater. 64 (2014) 326–332.
[119] J.-N. Zheng, S.-S. Li, X. Ma, F.-Y. Chen, A.-J. Wang, J.-R. Chen, J.-J. Feng, J. Power Sources 262 (2014) 270–278.
[120] B. Neppolian, V. Saez, J. Gonzalez-Garcia, F. Grieser, R. Gomez, M. Ashokkumar, J. Solid State Electrochem. 18 (2014) 3163–3171.
[121] Y. Liang, Y. Li, H. Wang, J. Zhou, J. Wang, T. Regier, H. Dai, Nat. Mater. 10 (2011) 780–786.
[122] J. Wu, C. Chen, Y. Hao, C. Wang, Colloids Surf. Physicochem. Eng. Asp. 468 (2015) 17–21.
[123] J. Yan, Z.J. Fan, T. Wei, W.Z. Qian, M.L. Zhang, F. Wei, Carbon 48 (2010) 3825–3833.
[124] Z. Wang, J. Sha, E. Liu, C. He, C. Shi, J. Li, N. Zhao, J. Mater. Chem. A 2 (2014) 8893–8901.
[125] Y.-L. Chen, Z.-A. Hu, Y.-Q. Chang, H.-W. Wang, Z.-Y. Zhang, Y.-Y. Yang, H.-Y. Wu, J. Phys. Chem. C 115 (2011) 2563–2571.
[126] I.Y.Y. Bu, R. Huang, Mater. Sci. Semicond. Process. 31 (2015) 131–138.
[127] A.G. El-Deen, N.A.M. Barakat, K.A. Khalil, M. Motlak, H.Y. Kim, Ceram. Int. 40 (2014) 14627–14634.
[128] H. Yin, S. Zhao, J. Wan, H. Tang, L. Chang, L. He, H. Zhao, Y. Gao, Z. Tang, Adv. Mater 25 (2013) 6270–6276.
[129] P. Gao, D.D. Sun, Chem. Asian J. 8 (2013) 2779–2786.
[130] W. Shu, Y. Liu, Z. Peng, K. Chen, C. Zhang, W. Chen, J. Alloys Comp. 563 (2013) 229–233.
[131] H. Huang, J. Fang, Y. Xia, X. Tao, Y. Gan, J. Du, W. Zhu, W. Zhang, J. Mater. Chem. A 1 (2013) 2495–2500.
[132] Y. Xiao, J. Qin, C. Hu, M. Cao, Mater. Chem. Phys. 141 (2013) 153–159.
[133] Y. Haldorai, A. Rengaraj, C.H. Kwak, Y.S. Huh, Y.-K. Han, Synth. Met. 198 (2014) 10–18.
[134] A. Ashkarran, B. Mohammadi, Appl. Surf. Sci. 342 (2015) 112–119.
[135] Z. Zhang, L. Ren, W. Han, L. Meng, X. Wei, X. Qi, J. Zhong, Ceram. Int. 41 (2015) 4374–4380.
[136] K.G. Lee, J.-M. Jeong, S.J. Lee, B. Yeom, M.-K. Lee, B.G. Choi, Ultrason. Sonochem. 22 (2015) 422–428.
[137] S. Wang, L. Zhang, Z. Xia, A. Roy, D.W. Chang, J.-B. Baek, L. Dai, Ange. Che. Int. Ed. 51 (2012) 4209–4212.
[138] Y. Zhang, K. Fugane, T. Mori, L. Niu, J. Ye, J. Mater. Chem. 22 (2012) 6575–6580.
[139] X. Wang, X. Li, L. Zhang, Y. Yoon, P.K. Weber, H. Wang, J. Guo, H. Dai, Science 324 (2009) 768–771.
[140] J. Han, J.Y. Cheon, S.H. Joo, S. Park, Solid State Sci. 33 (2014) 1–5.
[141] D.-Y. Yeom, W. Jeon, N.D.K. Tu, S.Y. Yeo, S.-S. Lee, B.J. Sung, H. Chang, J.A. Lim, H. Kim, Sci. Rep. 5 (2015) 09817.
[142] H. Fei, R. Ye, G. Ye, Y. Gong, Z. Peng, X. Fan, E.L.G. Samuel, P.M. Ajayan, J.M. Tour, ACS Nano 8 (2014) 10837–10843.
[143] Z.-S. Wu, A. Winter, L. Chen, Y. Sun, A. Turchanin, X. Feng, K. Muellen, Adv. Mater 24 (2012) 5130–5135.
[144] P. Chen, J.-J. Yang, S.-S. Li, Z. Wang, T.-Y. Xiao, Y.-H. Qian, S.-H. Yu, Nano Energy 2 (2013) 249–256.
[145] Z.-Y. Sui, Y.-N. Meng, P.-W. Xiao, Z.-Q. Zhao, Z.-X. Wei, B.-H. Han, ACS Appl. Mater. Interfaces 7 (2015) 1431–1438.
[146] Y. Zhou, C.H. Yen, S. Fu, G. Yang, C. Zhu, D. Du, P.C. Wo, X. Cheng, J. Yang, C.M. Wai, Y. Lin, Green Chem. 17 (2015) 3552–3560.
[147] H.F. Huang, C.L. Lei, G.S. Luo, Z.Z. Cheng, G.X. Li, S.L. Tang, Y.W. Du, J. Mater. Sci. 51 (2016) 6348–6356.
[148] T. Huynh Ngoc, C. Kocabas, S.H. Hur, Mater. Lett. 143 (2015) 205–208.
[149] M. Sahoo, K.P. Sreena, B.P. Vinayan, S. Ramaprabhu, Mater. Res. Bull. 61 (2015) 383–390.
[150] S. Dou, X. Huang, Z. Ma, J. Wu, S. Wang, Nanotechnol 26 (2015) 045402.
[151] F. Miao, B. Tao, P.K. Chu, Dalton Trans. 41 (2012) 5055–5059.
[152] H.F. Huang, L.Q. Xu, Y.M. Tang, S.L. Tang, Y.W. Du, Nanoscale 6 (2014) 2426–2433.

Alpha C.H. TSANG: His research field mainly deals with the three-dimensional graphene based materials, from preparation to the applications. Mainly the green energy and pollutant reduction.

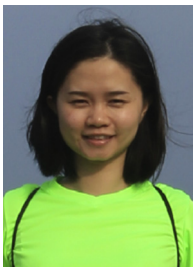

Holly Y.H. KWOK: She graduated at the University of Hong Kong with a BEng and MEng degree and is currently a PhD student in the Department of Mechanical Engineering at the University of Hong Kong. Her research interest focuses on the application of graphene in environmental and energy related field, from catalyst synthesis to device design.

Dennis Y.C. LEUNG: He is currently a professor of the Department of Mechanical Engineering at the University of Hong Kong. His research field is mainly in environmental protection and energy conversion. He has published more than 400 articles in this field including 220 + peer reviewed SCI journal papers. He has published more than 20 review articles in leading journals. His current h-index is 53 with total citations more than 10,000. He is one of the top 1% highly cited scientists in the world in energy field since 2010 until now.